Fire Research Note No. 620

FIRES IN A MODEL CORRIDOR WITH A SIMULATED COMBUSTIBLE CEILING.
PART I - RADIATION, TEMPERATURE AND EMISSIVITY MEASUREMENTS.

by

S. ATALLAH

FIRE RESEARCH STATION

F. R. Note No. 620
April 1966.

FIRES IN A MODEL CORRIDOR WITH A SIMULATED COMBUSTIBLE CEILING
PART I - RADIATION, TEMPERATURE AND EMISSIVITY MEASUREMENTS

by

S. Atallah

SUMMARY

An experimental study was performed in which a combustible ceiling was simulated by injecting town gas in porous burners covering a portion of the ceiling of a long duct with a primary gas fire at one end. Temperature profiles of the ceiling flame and radiometer and radiation pyrometer readings were taken at different points. The primary gas rate and the position and rate of ceiling gas were varied.

The data were used to calculate the emissivity and absorption coefficients of the ceiling flames by an approximate method which takes into account the variation of temperature across the flame. The flame emissivity was about 0.5. This high value was attributed to the high concentration of soot in the flame.

The addition of fuel at ceiling level by the injection of gas was found to increase flame length and the radiation falling on the floor considerably, particularly at low primary gas flow rates.

MINISTRY OF TECHNOLOGY AND FIRE OFFICES' COMMITTEE
JOINT FIRE RESEARCH ORGANIZATION

FIRES IN A MODEL CORRIDOR WITH A SIMULATED COMBUSTIBLE CEILING
PART I - RADIATION, TEMPERATURE AND EMISSIVITY MEASUREMENTS

by

S. Atallah

1. Introduction

This paper describes part of a programme designed to study the spread of fire in large enclosures. This particular phase of the study was concerned with changes in the level of thermal radiation to the floor due to the presence of a combustible ceiling in a long enclosure with a primary fire at one end. Earlier work by Hinkley[1] was performed in a large open bottom corridor with a wooden crib or gas fire at one end and a combustible ceiling of fibre insulation board. The difficulty with such experiments is that they are at an unsteady state, making systematic exploration of the patterns of flow and heat transfer difficult.

It was desired to simulate a burning ceiling by injecting town gas at an appropriate rate through porous burners covering a portion of the ceiling of a small corridor having no bottom with a primary gas fire burning at one end. The rate of flow and position of ceiling gas and the primary gas rate could thus be varied at will and the system allowed to reach a steady state at which time the desired temperatures and radiation intensity measurements could be taken. These data were to be used to provide information about the radiative properties of the flames within the corridor.

2. Radiation received by the floor of an enclosure

The intensity of radiation falling on a unit area of the floor of an enclosure with a burning ceiling depends on the geometrical configuration of the system and the level of radiation emitted by the primary and ceiling fires. As an example, consider the cubical enclosure shown in Figure (1) with a fire extending along one side wall, this primary fire having a source radiation intensity of 2.5 cal $cm^{-2}s^{-1}$, and a flame spreading on the whole ceiling with a variable intensity. The ceiling flame intensity is taken here as a step function of distance for simplicity. (The values chosen are based on data from experiments with gas fires in long corridors, see Table 2). Table 1 shows the calculated intensity of radiation received by elements A, B, C and D placed equidistantly along the axis of the floor as shown in Figure 1. It is seen that the ceiling fire contributes a significant amount to the total radiation falling on the floor.

Table 1

Intensity of Radiation in a Cubical Enclosure

Element	Radiation from primary fire cal $cm^{-2}s^{-1}$ M	Radiation from ceiling cal $cm^{-2}s^{-1}$ N	Total radiation intensity cal $cm^{-2}s^{-1}$ M + N	Percentage of total due to ceiling fire N/(M + N)
A	.88	.22	1.10	20
B	.63	.22	.85	26
C	.42	.21	.63	33
D	.30	.14	.44	32

Obviously, if the primary fire were less intense but was still able to set the ceiling on fire and the ceiling fire intensity remained the same, the percentage contribution of the ceiling radiation would be larger. If, for instance, the primary source radiated 1.5 cal $cm^{-2}s^{-1}$ (equivalent to a small wooden crib fire), element D would receive 0.18 cal $cm^{-2}s^{-1}$ from the primary source (which is not enough to ignite it if it were of wood) and 0.14 cal $cm^{-2}s^{-1}$ (44 per cent of the total) from the ceiling, which would increase the radiation to a hazardous level. It should also be pointed out that an increase in the rate of burning of the primary fire adds little from the vertical portion of the flame to the amount of radiation falling on a point on the floor but the resulting increase in hot gases deflected along the ceiling and eventually the burning ceiling itself contribute an increasing amount of radiation to the floor. This simplified picture of a fire in an enclosure is made much more complicated in actual fires by the presence (or absence) of ventilation and other modes of heat transfer.

3. Experiment

The experimental enclosure with pertinent dimensions is shown in Figure (2). The walls were constructed of 1.28 cm thick asbestos wood board and supported by a slotted angle-metal frame. Part of the ceiling was covered with three porous burners (35.5 x 35.5 cm) connected to the town gas mains supply. A similar burner served as the primary source of fire. The bottom of the corridor was open and was supported at a height of about one metre from the floor.

Six chromel-alumel thermocouples were placed less than 0.5 cm from the ceiling at distances of 18, 56, 89, 125, 165 and 231 cm from the closed end. These were used to obtain a horizontal temperature profile of the flame adjacent to the ceiling. Two additional thin wire (S.W.G. 40) thermocouples were placed at 81 and 178 cm. These two thermocouples could be moved vertically and were used to obtain the vertical temperature profile in the flame at these two points.

A narrow-angle total-radiation pyrometer was held manually pointing vertically upwards at distances of 65, 95 and 156 cm from the closed end during the experiment to find the intensity of radiation at these points. It was also occasionally sighted horizontally from the open end on the primary fire. A radiometer[2] was placed 33.5 cm below the ceiling at a point 119 cm from the closed end. A blackened block of asbestos board (11.4 x 11.4 x 1.28 cm) was placed at the same level and at a distance of 135 cm from the closed end. It had thermocouples embedded in the upper and lower surfaces.

The gas flow rate to the ceiling burners was measured using a rotameter and the primary gas rate was found using a calibrated orifice meter.

The primary gas burner was ignited, then one of the ceiling burners was turned on and both burners adjusted to the desired flow rates. The system was allowed to reach a steady state as indicated by the constancy of the thermocouple readings. This usually took between 30 and 45 minutes after which the experimental data were recorded.

4. Results

Typical experimental data are presented in Figures (3), (4) and (5). Primary and secondary gas flows are shown by insertion of values in l/s into the skeleton -/-/-/- where the first space gives the primary gas flow and the second, third and fourth spaces give the flow in burners A, B and C respectively. Figure (3) illustrates the changes in the horizontal flame temperature profile near the ceiling when gas was injected through the ceiling burners. There was a temperature drop in the vicinity of the ceiling burner where the cold gas was injected and this was also reflected in the pyrometer readings shown in Figure (4). Temperature profiles of the same tests taken at 81 and 178 cm are shown in Figure (5).

4.1. Radiometer Data

Table 2 summarizes the radiation measurements made when steady state conditions had been reached in all the runs. Figure (6) is a plot of the radiometer readings at different ceiling gas injection rates and positions. The position of the radiometer with respect to the ceiling burners is shown in Figure (2). The following general observations can be made:

1. The injection of gas in burner A produced about the same effect as an equivalent increase in primary gas rate on the radiometer readings.
2. Gas injection in burners B and C (further down stream from the primary fire) was not as effective in increasing the radiometer reading as injecting the same amount with the primary gas or in burner A. It seemed to be even less effective at higher ceiling gas rates.
3. In all cases of ceiling gas injection, there was an increase in the radiometer readings over the readings with no ceiling gas injection, particularly when gas was injected in burner A. As one would expect, the percentage increase in the radiometer reading was higher at the smaller primary gas flow rates and larger ceiling gas rates, the greatest increase being ~200 per cent for Test 2/1.4/-/-.

Table 2

Summary of Radiation Measurements

Test Identification*	Radiometer reading at 119 cm ($cal\ cm^{-2}s^{-1}$)	Radiation Pyrometer reading, $cal\ cm^{-2}s^{-1}$				Visual flame length, cm	Temperature of asbestos block °C	
		Primary flame	Distance, cm				Upper surface	Lower surface
			65	95	156			
4/-/-/-	.49		1.4	.96	.54	247	365	240
4/.8/-/-	.62	2.67	1.22	1.04	.70	257	410	265
4/-/.8/-	.57	2.53	1.46	1.00	.67	263	400	260
4/-/-/.8	.59	2.53	1.30	1.06	.65	269	395	260
4/1.4/-/-	.68		1.44	1.08	.76	276	415	255
4/-/1.4/-	.52		1.46	.86	.67	271	375	240
4/-/-/1.4	.50		1.32	.94	.58	271	375	240
3/-/-/-	.37	2.48	1.3	.83	.50	152	305	205
3/.8/-/-	.50	2.53	1.46	1.01	.67	249	370	235
3/-/.8/-	.44	2.43	1.27	.81	.50	246	345	230
3/-/-/.8	.42	2.48	1.27	.94	.47	239	335	225
2/-/-/-	.14		.6	.34	.24	81	172	130
2/.8/-/-	.33	2.60	.86	.74	.50	180	295	200
2/-/.8/-	.29		.72	.54	.42	221	290	200
2/-/-/.8	.22	1.64?	.76	.42	.54	76 + 114†	260	182
2/1.4/-/-	.43	2.36	.94	.88	.54	246	335	220
2/-/1.4/-	.35		.67	.72	.50	246	315	210
2/-/-/1.4	.30	2.58	.72	.50	.60	76 + 140†	312	212

*Test Identification: e.g. 4/-/-/.8 means that primary gas was fed at 4 l/s and ceiling gas at 0.8 l/s in burner C.
See Figure (2) for position of burners.

†Flame was discontinuous. The first length is the primary flame length and the second is the ceiling flame length starting at burner C.

The radiometer data of arbitrarily selected runs were checked for consistency with the radiation pyrometer readings. The bottom face of the flame seen by the radiometer was divided into smaller rectangular sections and the view factor between the radiometer and each section calculated. The average radiation intensity of each section was found from the pyrometer profile and the total radiation received by the radiometer evaluated and compared with actual readings (Table 3). The agreement is good considering that an average flame depth was used and that the radiation from the vertical sections of the wall seen by the radiometer was neglected. It was further assumed that the radiometer received 100 per cent of the radiation within an angle of 125° and nothing else[1].

Table 3

Calculated and Experimental Radiometer Readings

Test No.	Radiometer Reading cal $cm^{-2}s^{-1}$	
	Calculated	Experimental
4/-/-/-	.49	.49
4/.8/-/-	.56	.62
4/1.4/-/-	.50	.43
3/-/-/-	.42	.37
3/-/-/.8	.46	.42
2/-/-/-	.17	.14
2/1.4/-/-	.60	.68

4.2. Flame Length

Flame lengths were estimated visually and are plotted against primary gas flow rate per unit width of corridor in Figure 7. Data[1] from tests on wider corridors with larger flow rates are included and seem to agree well with the data on the small corridor. This figure also shows the large increase in flame length due to gas addition in burner A of the small corridor and due to a combustible ceiling of fibre board in one of the larger corridors. It should also be noted that the flame length is greater than it would have been had the ceiling gas been injected with the primary gas (indicated by arrows in Figure 7).

The flame length in the small corridor was not substantially changed upon altering the position at which ceiling gas was injected. The plotted data are limited to flames that did not reach far beyond the end of the corridor since it is difficult to predict what the length of the flame would be if the corridor had been extended.

4.3. Flame Depth

A flame rising from the floor of an enclosure is deflected by the ceiling and begins to drag with it a layer of air the depth of which increases with distance along the ceiling. Smoke injected in the experimental corridor displayed the dragged air pattern sketched in Figure 8. Temperature and velocity profiles taken on a larger corridor[1] were similar near the point of deflection, where there was a large amount of agitation, but differed downstream. Which depth is taken depends on whether one is interested in the aerodynamics of flow when the distance to the bottom of the dragged air layer is important, or whether one is interested in thermal radiation from the flame in which case the depth of the hot luminous layer is of significance.

In this study, an arbitrary temperature of 300°C was used to define the flame depth. It corresponded roughly to the bottom of the luminous layer and to the point at which there was a sharp change in the slope of the temperature profile. Whichever definition one chooses, consideration of the aerodynamics of the situation suggests that the depth of the hot gas layer below the ceiling ought to be some function of the following variables:

1. Flow rate of the primary gas per unit width of corridor.
2. Air entrainment in the primary flame, which is dependent on the clearance between the burner and the ceiling and the degree of turbulence of the flame (itself dependent on primary gas velocity).
3. The average absolute temperature of the hot gas layer.
4. The temperature difference between the hot gas layer and the ambient air.

Table 4 gives values of the flame depth at two different positions in the corridor.

Table 4

Flame depth, temperature and radiative properties

Test Identification	Distance									
	81 cm					178 cm				
	Flame depth cm	Flame emissivity	Absorption coefficient cm^{-1}	Flame temperature T_F °K	bC_s, relative soot concentration	Flame depth cm	Flame emissivity	Absorption coefficient cm^{-1}	Flame temperature T_F °K	bC_s, relative soot concentration
4/-/-/-	18.2	.53	.041	1032	.034	10.9	.31	.035	863	.035
4/.8/-/-	23.1	.68	.048	1004	.045	13.1	.29	.026	938	.021
4/-/.8/-	18.6	.62	.053	1035	.047	11.7	.38	.041	938	.038
4/-/-/.8	24.1	.70	.050	1003	.047	12.9	.41	.042	888	.044
4/1.4/-/-	13.6	.67	.082	1022	.076	13.6	.34	.031	1010	.024
4/-/1.4/-	18.0	.47	.035	1045	.028	12.7	.27	.022	978	.014
4/-/-/1.4	17.5	.41	.031	1048	.023	12.7	.20	.016	945	.008
3/-/-/-	17.1	.45	.035	1012	.029	11.7*	(.74)	(.120)	790	(.19)
3/.8/-/-	17.8	.65	.059	1026	.053	12.7	.71	.098	880	.120
3/-/.8/-	17.0	.48	.038	1008	.032	12.1	.38	.038	863	.040
3/-/-/.8	16.5	.60	.055	1007	.050	12.1	.20	.017	848	.011
2/-/-/-	12.4	(.04)	(.003)	839	nil	8.9*	(.54)	(.086)	692	(.17)
2/.8/-/-	16.0	.57	.052	925	.055	11.4	.20	.018	873	.011
2/-/.8/-	15.2	.41	.035	899	.035	10.4	.05	.005	864	nil
2/-/-/.8	15.6	(.83)	(.12)	788	(.19)	11.9	.05	.004	940	nil
2/1.4/-/-	17.5	.33	.024	1038	.016	11.7	.15	.013	953	.003
2/-/1.4/-	18.0	.39	.027	925	.024	11.4	.03	.002	978	nil
2/-/-/1.4	16.8	.26	.018	889	.013	11.9	.20	.017	968	.008

Numbers in parenthesis may be in error

* No luminous flame was present at 178 cm

An analysis of variance showed that the position and rate of ceiling gas injection had no significant effect on depth measured at 81 and 178 cm but that there was a statistically significant increase in depth due to an increase in primary gas rate. There was also a significant effect on depth at 81 cm due to an interaction between the primary and secondary gases. This could be attributed to the single low value of depth in Test 4/1.4/-/-. If one bars experimental error, this low value may have been due to the probe position which, at 81 cm, was immediately after the ceiling gas from burner A had pushed the horizontal primary gas flame downward producing an inverted weir (waterfall) effect with a shallow region immediately afterwards.

4.4. Emissivity of Ceiling Flames

4.4.1. Theoretical Derivation

Consider a ceiling below which there is a grey flame of thickness d radiating downwards towards a narrow-angle total radiation pyrometer (Figure 9). If the soot and combustible gases concentrations are assumed constant across the flame and if the temperature profile is known, one should be able to calculate an overall flame emissivity following the procedure suggested below. This method is a combination of the traverse method given by Beer and Claus[3] and the Schmidt method[4].

A total radiation pyrometer sighted at the flames and ceiling would give a reading P which is equal to the sum of radiation received directly from all the elements Δx of the flame and the radiation from the ceiling through the flame (See Figure 9).

The radiation from a typical element of flame Δx which reaches the pyrometer is

$$P_{\Delta x} = \epsilon_{\Delta x} \quad R_x \quad e^{-kx} \qquad \ldots\ldots\ldots (1)$$

where $R_x = \sigma T_x^4$ (cal $cm^{-2}s^{-1}$)

σ = Stefan-Boltzmann constant (= 1.37×10^{-12} cal $cm^{-2}s^{-1}{}^{o}K^{-4}$)

T_x = absolute temperature of element Δx (^{o}K)

k = an overall attenuation, absorption or extinction coefficient (cm^{-1})

x = distance from the bottom of the flame (cm)

$\epsilon_{\Delta x}$ = emissivity of element Δx (dimensionless)

The emissivity of element Δx is given by

$$\epsilon_{\Delta x} = 1 - e^{-k \Delta x} \qquad \ldots\ldots\ldots (2)$$

which, in the limit as $\Delta x \rightarrow 0$ becomes $k\ dx$.

The total radiation received by the pyrometer from the flame and the ceiling is given by

$$P = R_w\ e^{-kd} + \int_0^d k\ R_x\ e^{-kx}\ dx \qquad \ldots\ldots\ldots (3)$$

where R_w = radiation from the ceiling or background wall which, if black, would be σT_w^4 (cal $cm^{-2} s^{-1}$)

T_w = wall or ceiling temperature (^oK)

d = flame depth (cm)

In order to obtain k from equation (3), a tedious trial and error solution is necessary in which a value is assumed for k and the right hand side evaluated by graphical means and compared with the measured value of P. In cases where the temperature profile is flat or not heavily lopsided, an average $\overline{R}_x$ may be used without much error and equation (3) integrated into:

$$P = R_w\ e^{-kd} + \overline{R}_x\ (1 - e^{-kd}) \qquad \ldots\ldots\ldots (4)$$

where $$\overline{R}_x = \frac{1}{d} \int_0^d R_x\ dx = \frac{\sigma}{d} \int_0^d T_x^4\ dx \qquad \ldots\ldots\ldots (5)$$

By simple algebraic manipulation of equation (4), it can be shown that the flame emissivity, ϵ_F is given by

$$\epsilon_F = 1 - e^{-kd} = \frac{P - R_w}{\overline{R}_x - R_w} \qquad \ldots\ldots\ldots (6)$$

If the pyrometer is sighted on a cold target in the ceiling, R_w becomes negligible and the emissivity is given by

$$\epsilon_F = \frac{P}{\overline{R}_x} \qquad \ldots\ldots\ldots (7)$$

An average flame temperature, T_F, can be defined by

$$T_F = \left\{\frac{\overline{R_x}}{\sigma}\right\}^{\frac{1}{4}} \qquad \ldots\ldots\ldots (8)$$

4.4.2. The Schmidt Method

The Schmidt method[4] normally used for finding luminous flame emissivity in furnaces requires readings with a total radiation pyrometer viewing through the flame (a) the hot furnace wall (assumed to behave as a black body) and (b) a cold target. It also requires the measurement of the wall temperature T_w. The flame emissivity is then calculated from

$$\epsilon_F = 1 - \frac{P_2 - P_1}{\sigma T_w^4} \qquad \ldots\ldots\ldots (9)$$

where P_1 = pyrometer reading when sighted at a cold target behind the flame = $\epsilon_F \sigma T_F^4$

P_2 = pyrometer reading when sighted at the hot furnace wall = $P_1 + \sigma T_w^4 \tau_F$

τ_F = flame transmittance for radiation from the hot background = $1 - \epsilon_F$

The Schmidt method, like the integral method described in section 4.4.1. above, assumes[5] that the flame is grey and causes negligible scattering and that the spectrum of wall radiation is continuous. Its major drawback is that it assumes the flame temperature to be uniform along the beam and equal to the wall temperature. It has the advantage of eliminating the need for flame temperature estimation since it is not used in calculating ϵ_F.

4.4.3. Experimental values of flame emissivity

The flame emissivity was calculated by equations (5) and (6) and is given in Table 4. The corresponding values of the absorption coefficient, k, and the flame temperature, T_F, are also tabulated. In performing these calculations, the following assumptions were made:

1. The ceiling behaved as a black body. This was a reasonable assumption because of the accumulation of soot on the ceiling.
2. The ceiling thermocouples gave an accurate measure of the wall temperature. Although the thermocouples extended slightly (<0.5 cm) below the ceiling, soot tended to build up to the level of the thermocouples. However, the thermocouples themselves accumulated some soot, the insulating properties of which may have affected the thermocouple readings.
3. The flame temperature was accurately measured by the thin wire thermocouples. This was probably the largest source of error in the calculations. An increase of 50°C in the average flame temperature of run 3/-/.8/- at 178 cm for instance, reduces the calculated emissivity from 0.38 to 0.27. The error in emissivity would be smaller for runs with higher flame temperatures. It is doubtful that the difference between the true flame temperature and the thermocouple temperature exceeded 50°C because of the small diameter of the thermocouple wire which increased the convective heat transfer coefficient from the flame to the thermocouple thus giving a more accurate value for flame temperature.

The radiation pyrometer readings, P, were found by plotting the experimental values versus distance and interpolating at 81 cm and extrapolating to 178 cm. This presented additional unpredictable errors in the calculated values of ϵ_F and k at 178 cm and in a few cases at 81 cm because the shape of the curve was uncertain.

In general, the emissivity and absorption coefficients at 81 cm were higher than those at 178 cm.

It is unwise to make any further generalizations concerning the effects of primary gas rate and ceiling gas rate and position on emissivity and adsorption coefficients at this stage of the study because of the possible experimental errors mentioned above.

4.4.4. Comparison of the Schmidt and Integral Methods

Temperature profiles and radiation data obtained[1] by sighting a total radiation pyrometer on the hot ceiling and on a cold target in the ceiling of an 80 cm wide corridor were used to compare the two integral methods for calculating flame emissivity (i.e. equations (6) and (7)) with the Schmidt method. The emissivities, flame depths and absorption coefficients found for town gas flames are given in Table 5.

Table 5

Radiative Properties of Flames in 80 cm Corridor

Test No.	Gas rate (l/s)	d (cm)	Flame emissivity			k## (cm^{-1})
			Schmidt method	Integral Method		
				eq. (6)	eq. (7)	
117*	10	12.1	.49	.50	.47	.054
114	20	24.1	.35	.49	.42	.023
115	30	27.9	.45	.56	.49	.025
165†	20	37.0	.36	.64	.52	.020
166†	28	41.9	.57	.57	.55	.020

*pyrometer sighted on non-luminous sooty combustion gases.

†23 cm curtain was added at the end of the corridor to increase layer depth.

##averaged values for the three methods.

Values of the emissivity found by the Schmidt method[1] are plotted with those found by the two integral methods against flame depth in Figure 10. There was a statistically significant difference between the three methods. The integral method using the hot ceiling data gave the highest values of emissivity and the lowest were obtained by the Schmidt method. The integral methods seemed to give more consistent and less scattered results than the Schmidt method, probably because they can deal more effectively with large temperature gradients in the luminous flame.

For both corridors, when solid flames were present below the ceiling, the flame emissivity was about 0.5. This is remarkably high compared with the value of about 0.15 obtained by Heselden[6] for a 30 cm thick flame of town gas in open air from a burner similar to those employed in this study. The explanation probably lies in the very low mixing of air with the ceiling flame. It is well known that more soot is produced and luminous radiation is increased in coke-oven gas flames if the rate of entrainment of air is delayed[7].

4.5. Soot Concentration in the Flame

The total emissivity of the flame ϵ_F can be attributed to the presence of soot and gaseous combustion products. Blokh[8] gives the following equation for the emissivity of a sooty flame

$$\epsilon_F = 1 - e^{-\eta K d} \quad (1 - \epsilon_g) \qquad \ldots\ldots (10)$$

where η = a constant

$K = (1.56 \times 10^{-3} T_F - .64) \frac{\mu}{\gamma}$

μ = gravimetric concentration of soot

γ = specific weight of soot

ϵ_g = emissivity of gaseous combustion products (H_2O and CO_2)

Equation (10) can be rewritten in the form

$$\epsilon_F = 1 - e^{-kd} = 1 - (1 - \epsilon_g)\, e^{-bC_s d (1.56 \times 10^{-3} T_F - 0.64)} \ldots\ldots (11)$$

where b = a constant

C_s = soot concentration

Equation (11) can be rearranged to give

$$b\, C_s = \left[k + \frac{\ln (1 - \epsilon_g)}{d}\right] \Big/ (1.56 \times 10^{-3} T_F - .64) \qquad \ldots\ldots (12)$$

The emissivity of combustion gases ϵ_g can be calculated if their partial pressures or concentrations were measured. This was not done in this experiment. The maximum contribution of gaseous combustion products to flame emissivity is when combustion is complete and when air is present in stoichiometric proportions. By using the average flame temperature, the appropriate town gas composition* and the method described by Hottel[9], maximum values of ϵ_g were calculated at different flame thicknesses. Substituting these values in equation (12) gave bC_s, which, in this case, was a measure of the minimum amount of soot present in the flame.

---

*The average gas composition in Boreham Wood during the first two months of 1966 was approximately CO_2 = 5 per cent, O_2 = 1.5 per cent, $C_n H_n$ = 4.5 per cent, H_2 = 44 per cent, CO = 20.5 per cent, $C_n H_{2n+2}$ = 14.5 per cent, N_2 = 10 per cent.

This term is also listed in Table 4. Considering the accumulated errors in the results and the assumptions made, no generalizations will be attempted concerning soot concentration at this stage of the study beyond pointing out the possibility of using this method for comparing soot concentrations in flames.

5. Conclusions

1. Injection of gas through any of the ceiling burners increased the intensity of radiation at the radiometer. The increase was greatest when gas was injected in Burner A and in this case the increase was about the same as that produced by an equivalent increase in primary gas rate.

2. The experiments indicate that the presence of a combustible ceiling in a corridor with a fire at one end should increase flame length and radiation falling on the floor considerably, particularly when the primary fire is small.

3. It was possible to correlate town gas flame lengths in corridors of different widths by plotting flame length L (cm) against primary gas flow rate per unit width of corridor P (cm^2/s). For $55 < P < 290$

$$L \doteq 2.36 \quad P - 46$$

4. An integral method for the determination of the emissivity of flames with large temperature gradients has been devised and found to give more consistent results than the Schmidt method.

5. Town gas flames enclosed by a ceiling and two sides give an average absorption coefficient for a vertical path of .022 cm^{-1}. This value leads to much higher emissivities than those obtained for town gas flames in the open.

6. Recommendations

1. It is recommended that a larger, geometrically similar corridor model be constructed and used to investigate the conditions for thermal and aerodynamic similarity between the two systems.

2. In order to use information obtained from gas fires in small enclosures for large scale fires, the radiative properties of the luminous flames of other combustibles should be investigated. The emissive properties of liquid fuel flames have been partially investigated[10] but there is a lack of information on the radiative properties of flames from solid fuels. As a start, it is suggested that a systematic study be conducted of the radiative properties of wood crib fires.

3. The results of this study indicate that the presence of an enclosure around a gas burner may change the radiative properties of the flame considerably. It is recommended that a laboratory study be made of this employing more than one method for measuring the emissivity of the luminous flame.

7. Acknowledgements

The author wishes to thank Dr. P. H. Thomas, Mr. A.J.M. Heselden and Mr. P. L. Hinkley for their instructive comments and discussions. Miss A. I. Wadley and Mr. H.G.H. Wraight helped in the experimental measurements.

8. References

1. HINKLEY, P. L. Unpublished data.
2. McGUIRE, J. H. and WRAIGHT, H. G. H. J.Sci.Instr. (1960) 37, 128.
3. BEER, J. M. and CLAUS, J. J. Inst. Fuel (1962) 35, 437-443.
4. SCHMIDT, H. Ann. Phys. (1909) 29, 971-1028.
5. WEEKS, O. J. and SAUNDERS, O. A. J. Inst. F. (1958) 31, 247-258.
6. HESELDEN, A. J. M. Private communication.
7. THRING, M. W. Methods of increasing the emissivity of coke-oven gas flames. J. Inst. Fuel (1956) 29, 27-30
8. BLOKH, A. G. Thermal Engineering (1964) 11, 4, pp. 32-38. Translated from Toploenergetika (1964) 11, 4, pp. 26-30.
9. HOTTEL, H. C. Chapter IV in McAdams W. H., "Heat Transmission", 3rd ed., McGraw-Hill Book Co., New York (1954).
10. RASBASH, D. J., ROGOWSKI, Z. W. and STARK, G.W.V. Fuel (1956) 35, 94-107.
11. McADAMS, W. H. "Heat Transmission", 3rd ed., McGraw-Hill Book Co., New York (1954) p. 180.

APPENDIX I

The Asbestos Board Block Data

The blackened asbestos board block was used to examine the feasibility of employing it to replace the radiometer and to obtain a measure of heat losses by convection. The consistency of the data was checked by using the upper and lower surface temperatures of the block to evaluate the convective heat transfer coefficients for the two surfaces. These values were compared with those predicted by equations in the literature.

A heat balance on the upper surface of the block gives

$$\epsilon_a \ (R - \sigma T_u^4) = \frac{k\,(T_u - T_b)}{\Delta x} + h_u\,(T_u - T_a) \qquad \ldots\ldots\ldots \text{(A-1)}$$

where ϵ_a = emissivity of blackened asbestos board, taken as 0.9.

R = radiometer reading, assumed to be equal to the intensity of radiation falling on the block. This is not exactly true since the block sees through an angle of 180° but this is partially offset by the fact that the block is 16 cm further downstream from the hot region of the corridor and its view factor, and thus the intensity of radiation falling upon it, will be less than if it were placed at the radiometer position.

T_u = upper surface temperature ($^\circ$K)

T_b = bottom surface temperature ($^\circ$K)

T_a = ambient temperature, taken as 303°K for the gases above the upper surface

k = thermal conductivity of asbestos board.

$\simeq .0265 \times 10^{-5} t(^\circ C) + .077 \times 10^{-3}$ (cgs units) (extrapolated from NPL data)

Δx = thickness of the block (cm)

h_u = convection heat transfer coefficient to the upper surface (cal $deg C^{-1} cm^{-2} s^{-1}$).

Calculated values of h_u varied between $.179 \times 10^{-3}$ and $.534 \times 10^{-3}$ with the higher values corresponding to the higher primary gas flow rates. McAdams[11] suggests the following empirical equation for natural convection from a hot horizontal surface to air

$$h_u = .3625 \times 10^{-4} (T_u - T_a)^{\frac{1}{3}} \qquad \ldots\ldots\ldots (A\text{-}2)$$

This equation gives corresponding values ranging between $.189 \times 10^{-3}$ (Test 2/-/-/-) and $.264 \times 10^{-3}$ (Test 4/1.4/-/-).

The disagreement at the higher gas rates cannot be attributed to the inadequacy of McAdams' equation since the smoke generated by a smouldering piece of wood showed no sign of horizontal bulk movement of air near the surface of the block. Major sources of error are:

1. The value of thermal conductivity used. The thermal properties of asbestos board vary a great deal with density and manufacturer.
2. The fact that the calculation of h_u involves differences between numbers of the same order of magnitude.
3. The assumed value of the emissivity of asbestos.
4. Edge effects and heat losses to the metal supports.

Heat losses by convection from the upper surface ranged between 17 and 35 per cent, averaging about 28 per cent.

Convection heat transfer coefficients were also calculated for the bottom surface by writing the following heat balance:

$$k \frac{(T_u - T_b)}{\Delta x} = \epsilon_a \sigma (T_b^4 - T_a^4) + h_b (T_b - T_a) \qquad \ldots\ldots\ldots (A\text{-}3)$$

where T_a was taken as $293^{\circ}K$ for the ambient air near the bottom surface

h_b = bottom convection heat transfer coefficient (cal $cm^{-2}{}^{\circ}C^{-1}s^{-1}$)

Experimental values of h_b ranged between $.458 \times 10^{-4}$ and 1.65×10^{-4} cal $cm^{-2}{}^{\circ}C^{-1}s^{-1}$. The equation suggested by McAdams for this case is

$$h_b = .4425 \times 10^{-4} \left\{\frac{T_b - T_a}{L}\right\}^{\frac{1}{4}} \qquad \ldots\ldots (A\text{-}4)$$

where L = characteristic length of block (cm)

This equation gives values of h_b ranging between $.78 \times 10^{-4}$ (Test 2/-/-/-) and $.952 \times 10^{-4}$ (Test 4/.8/-/-). Again, the wide variation in experimental data could be attributed to the same sources of error listed above, particularly the heat losses to the metal supports which were attached to the bottom surface. The heat losses from the bottom surface by convection ranged between 12 and 52 per cent, averaging about 29 per cent.

This experiment showed that the asbestos block cannot be used to replace a radiometer where accuracy is desired. However, upon plotting the radiometer reading versus T_u^4 (see Figure 11), a surprisingly good straight line was obtained which suggests the possibility of calibrating the asbestos block against a standard radiometer and then using it (under similar conditions) in steady state systems where simplicity and ruggedness are desired.

APPENDIX II

A Useful Plot of the Equation: $\epsilon = 1 - e^{-kd}$

In preparing Table (4), it was found that the graphical presentation of the equation

$$\epsilon = 1 - e^{-kd} \qquad \ldots\ldots(A\text{-}5)$$

would be helpful in performing the calculations and useful in general.

Equation (A-5) was rearranged in the form

$$-\ln (1 - \epsilon) = kd \qquad \ldots\ldots(A\text{-}6)$$

and a plot of k versus d with ϵ as a parameter was prepared (Figure 12).

Given a value of k (typical approximate values[10] are shown on the plot) one can easily find the size of a fire behaving as a black body ($\epsilon \doteq 0.99$) or the emissivity of a flame of known thickness.

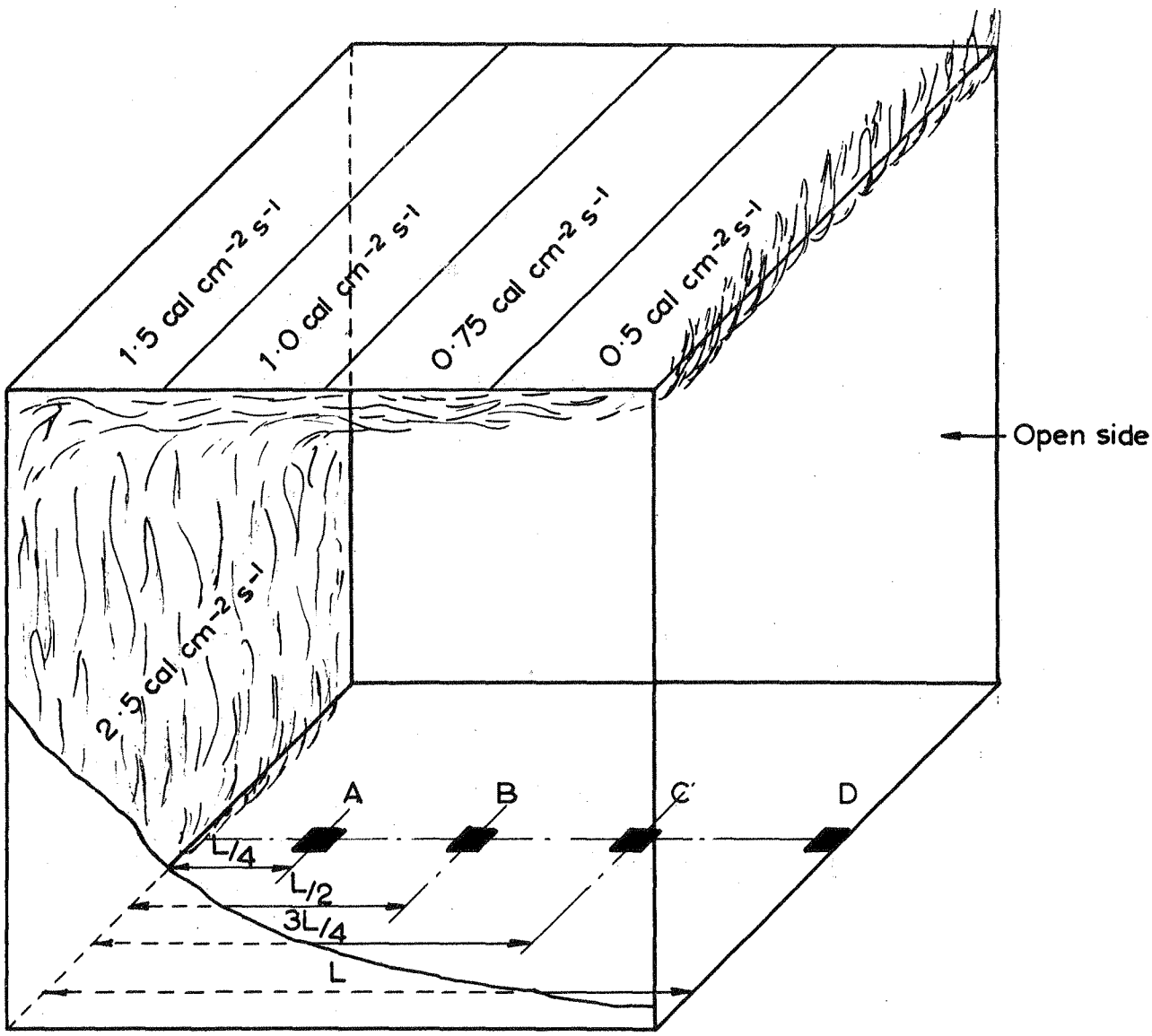

FIG. 1. CUBICAL ENCLOSURE WITH PRIMARY AND CEILING FIRE

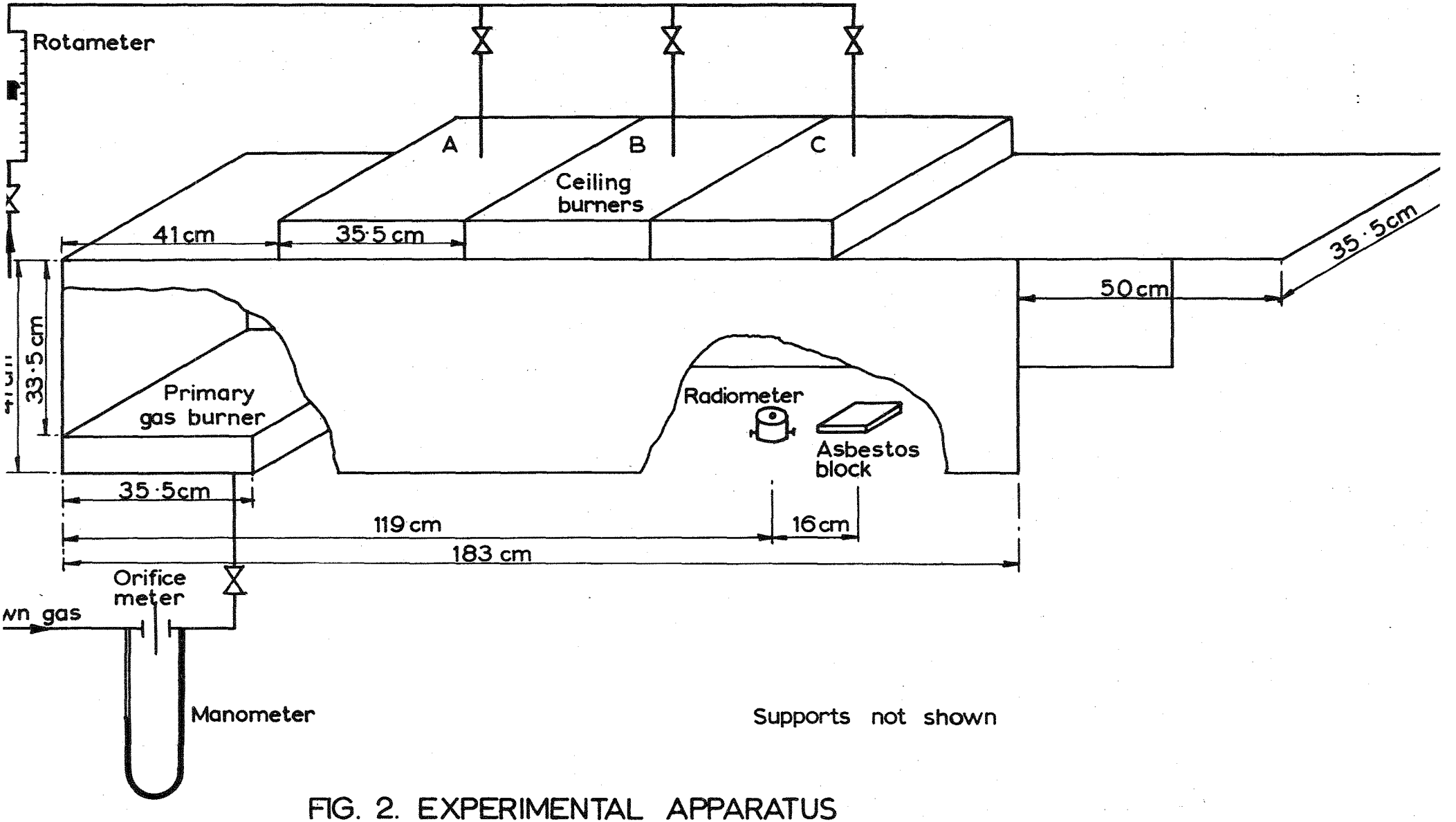

FIG. 2. EXPERIMENTAL APPARATUS

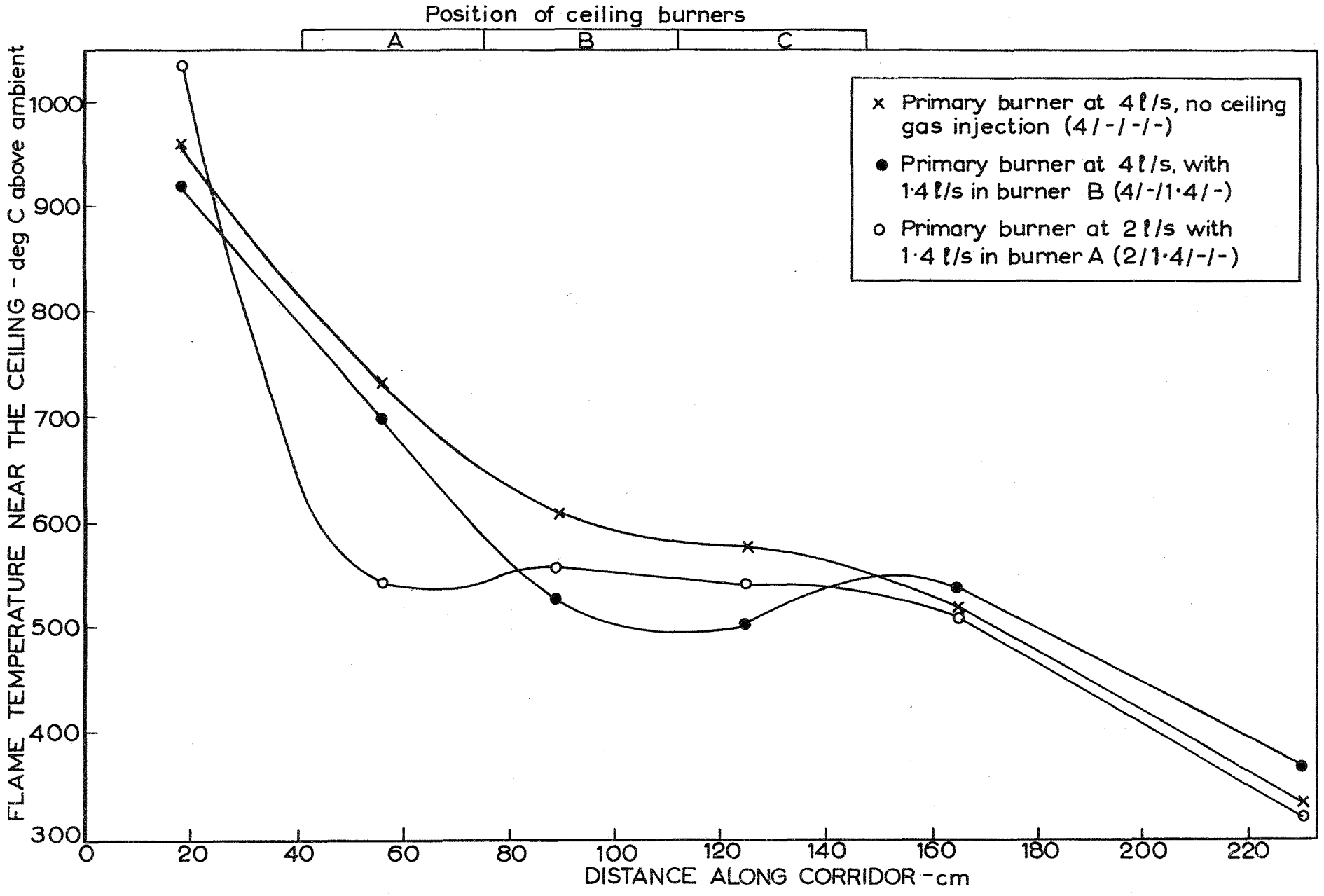

IG. 3. TYPICAL TEMPERATURE PROFILES ALONG CORRIDOR WITHIN 0·5cm OF THE CEILING

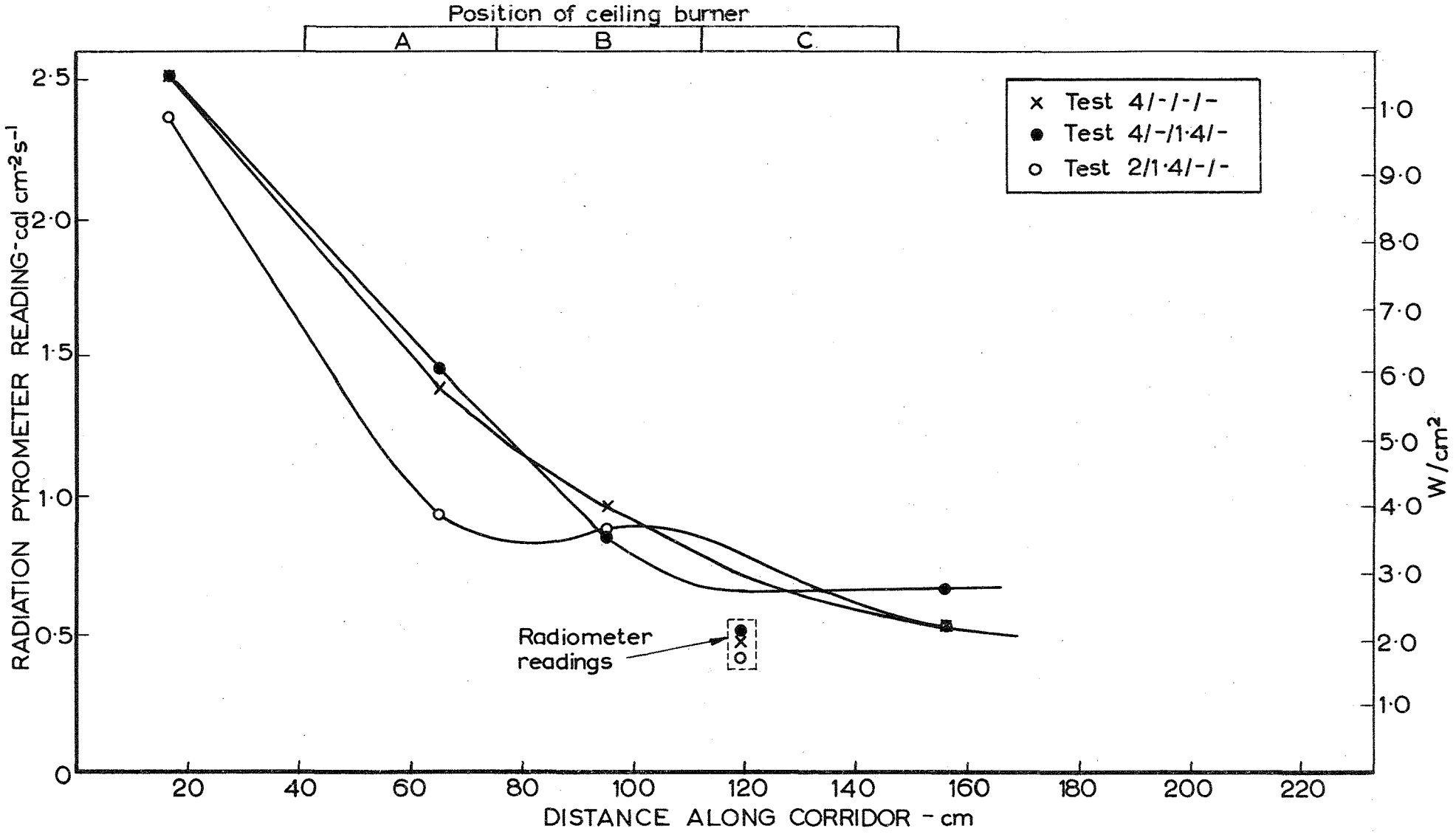

FIG. 4. TYPICAL RADIATION PYROMETER AND RADIOMETER READINGS

1/6864 F.R.620

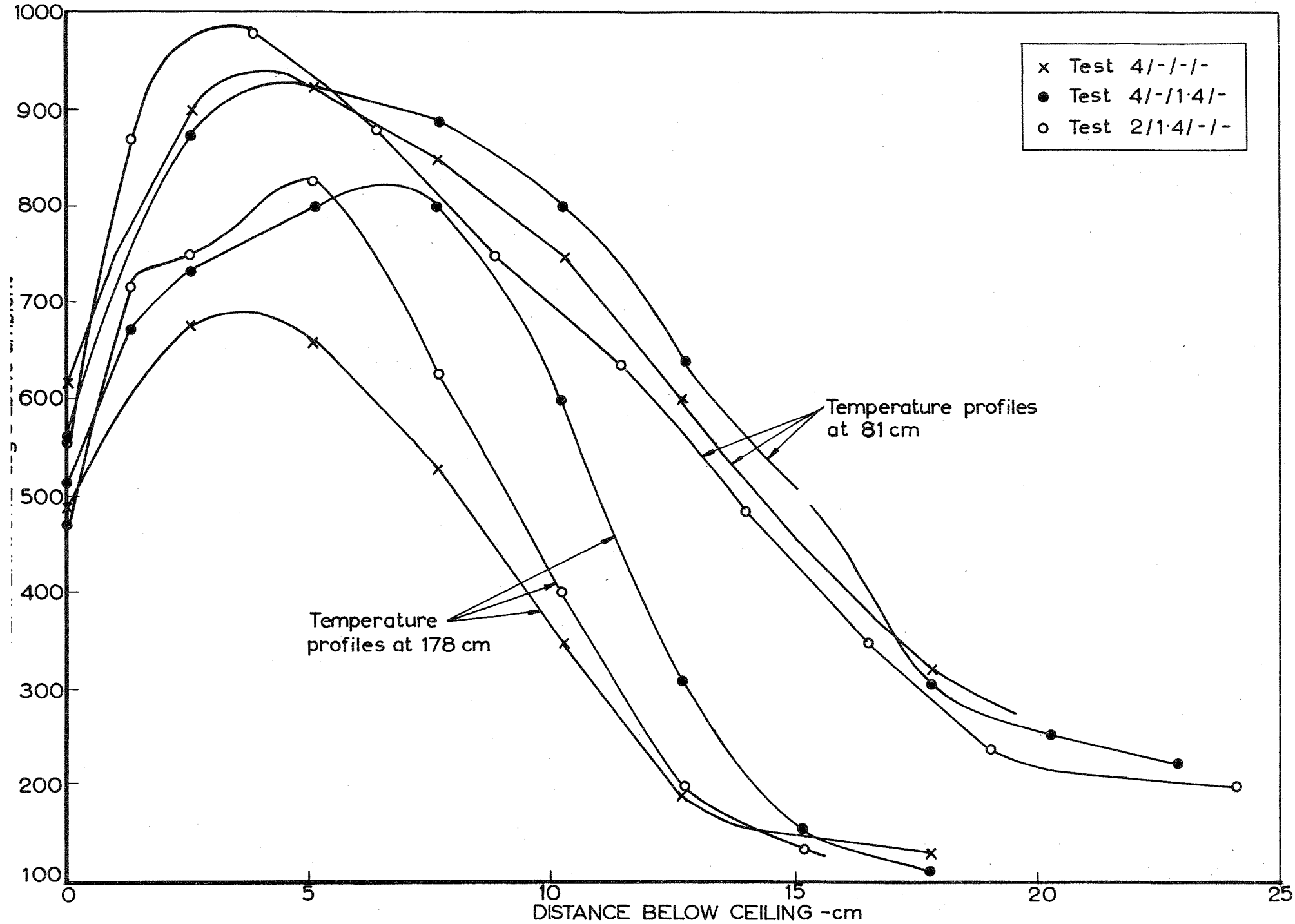

FIG. 5. TYPICAL TEMPERATURE PROFILES OF THE FLAMES BELOW THE CEILING

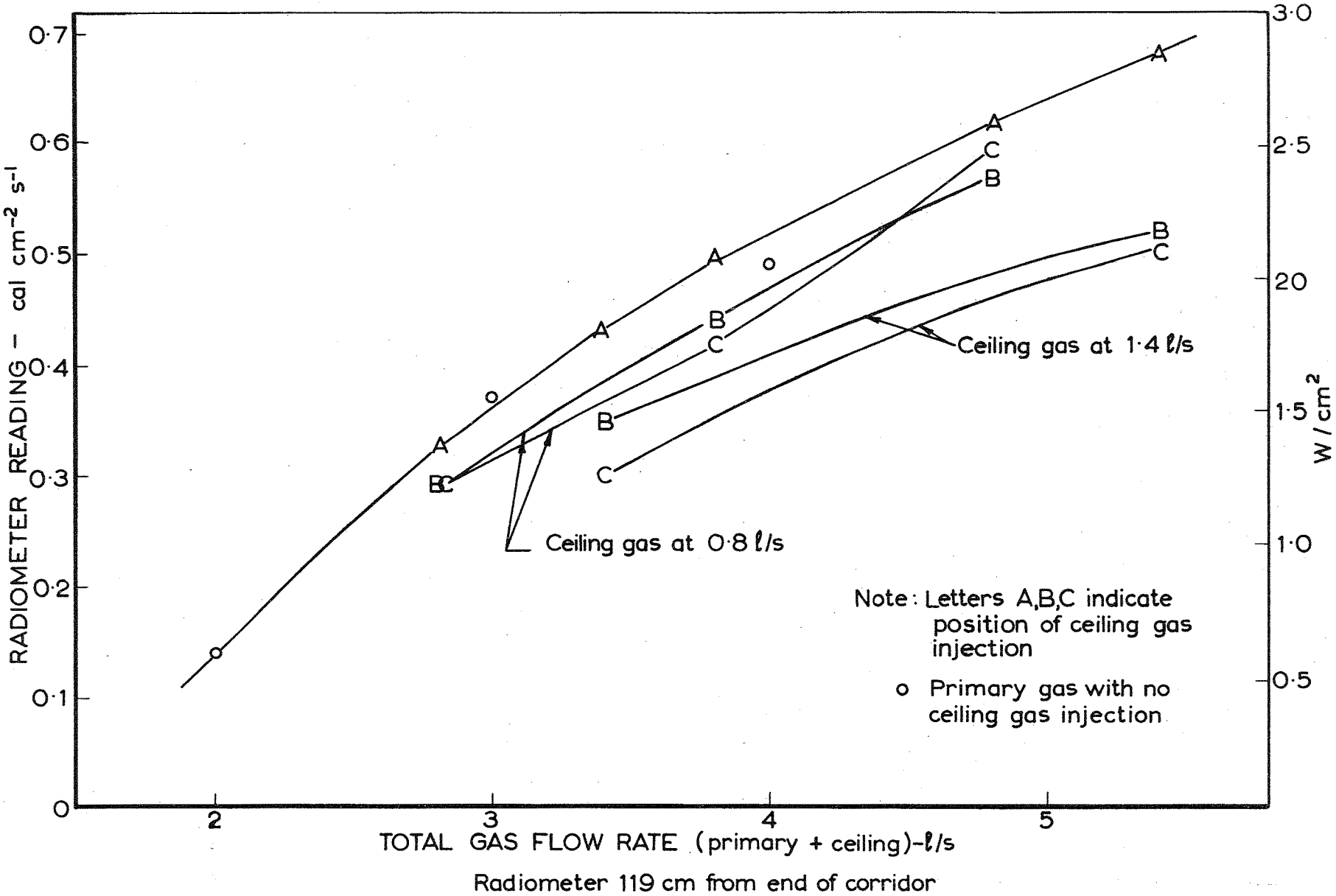

FIG. 6. RADIOMETER RESPONSE TO CEILING GAS INJECTION AT DIFFERENT RATES AND POSITIONS.

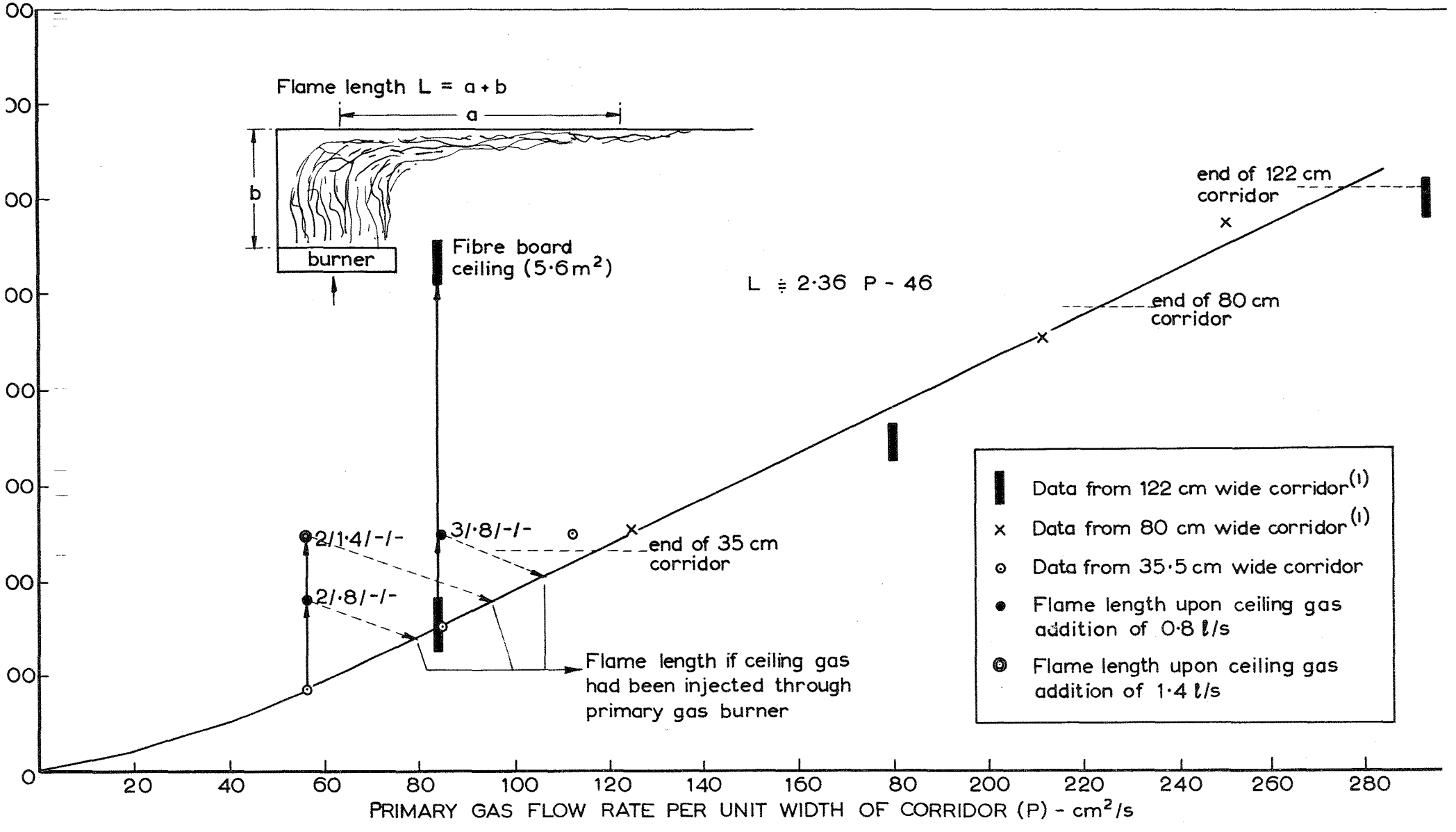

FIG. 7. FLAME LENGTH AND GAS FLOW RATE PER UNIT WIDTH OF CORRIDOR

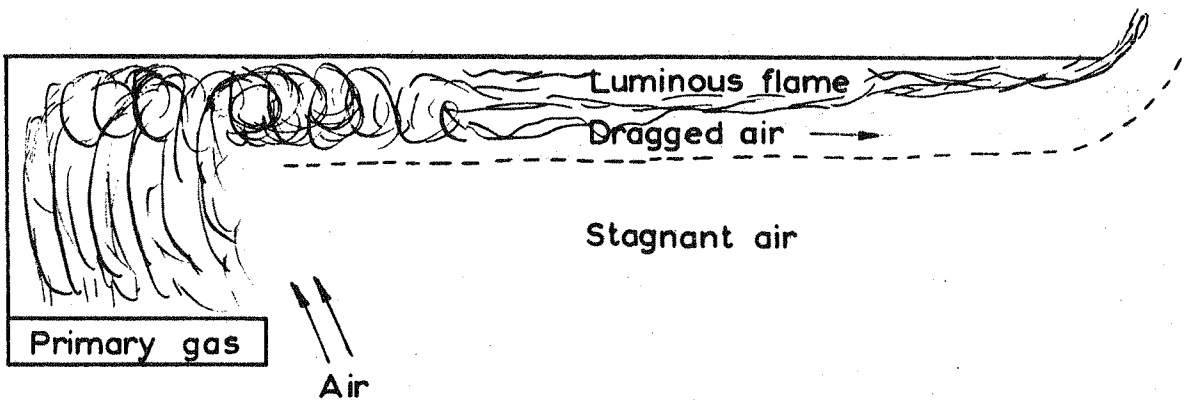

FIG. 8. HOT GAS LAYERS BELOW THE CEILING

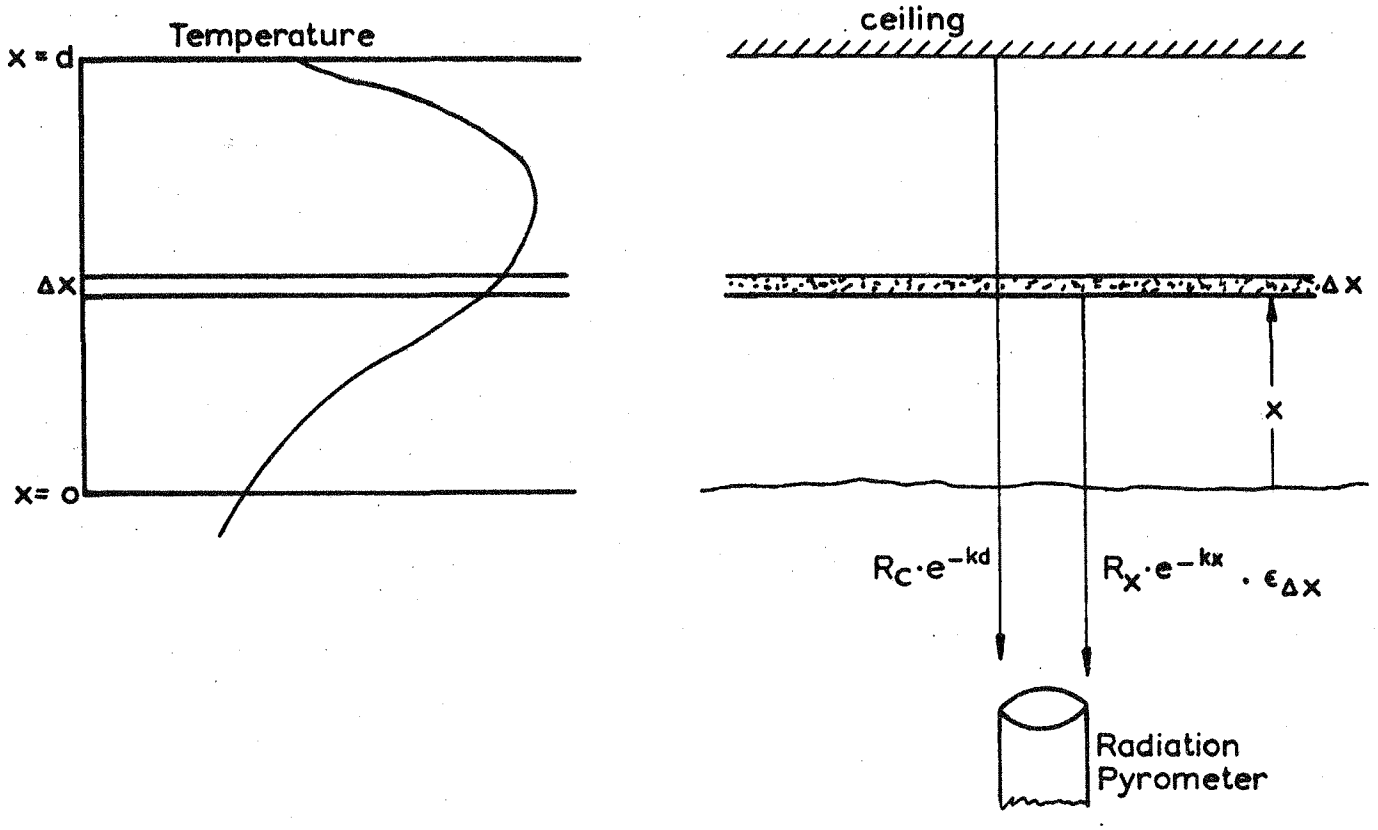

FIG. 9. THEORETICAL MODEL FOR RADIATION FROM A CEILING FLAME

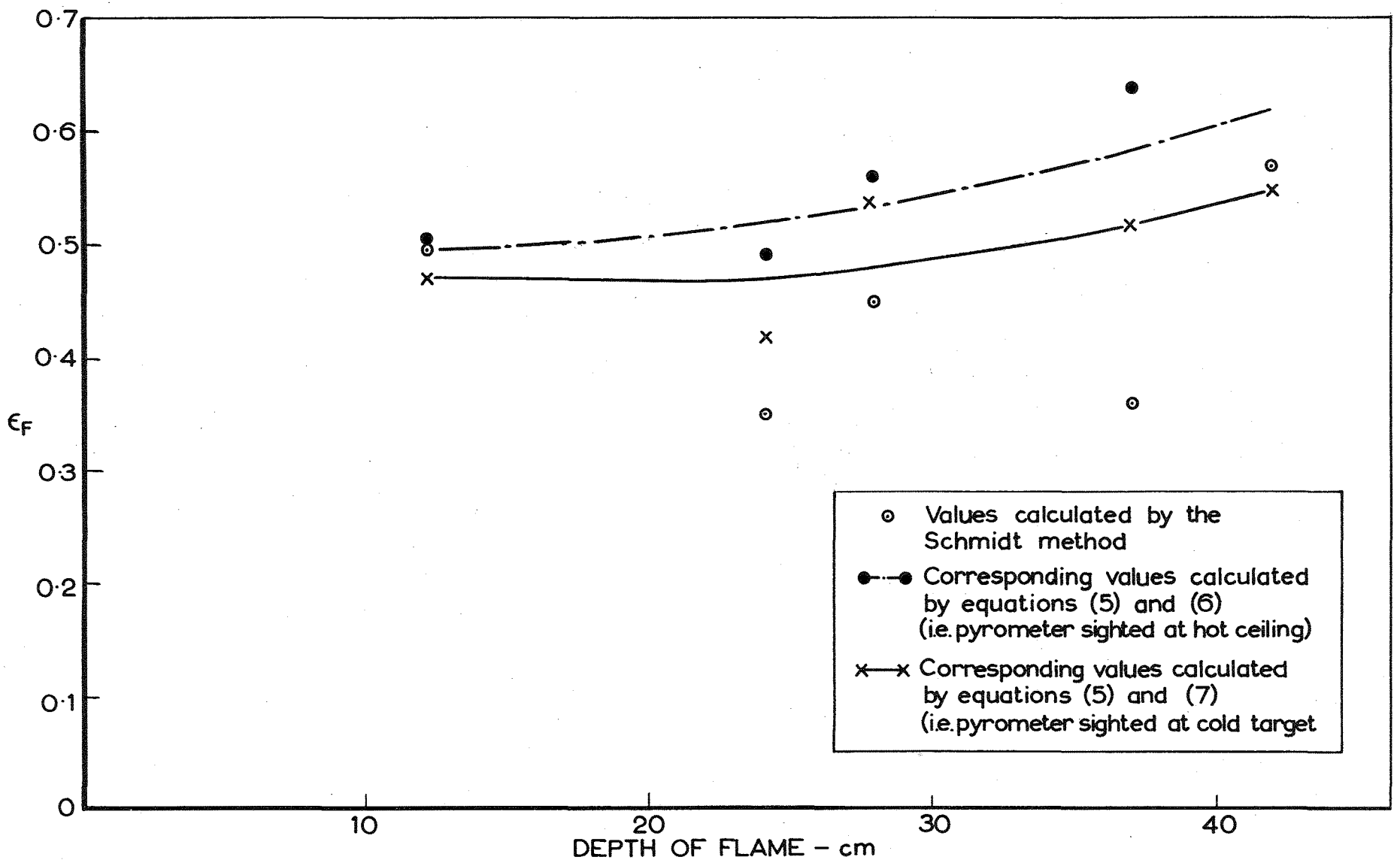

FIG. 10. FLAME EMISSIVITY AND DEPTH OF FLAME (80 cm CORRIDOR DATA)

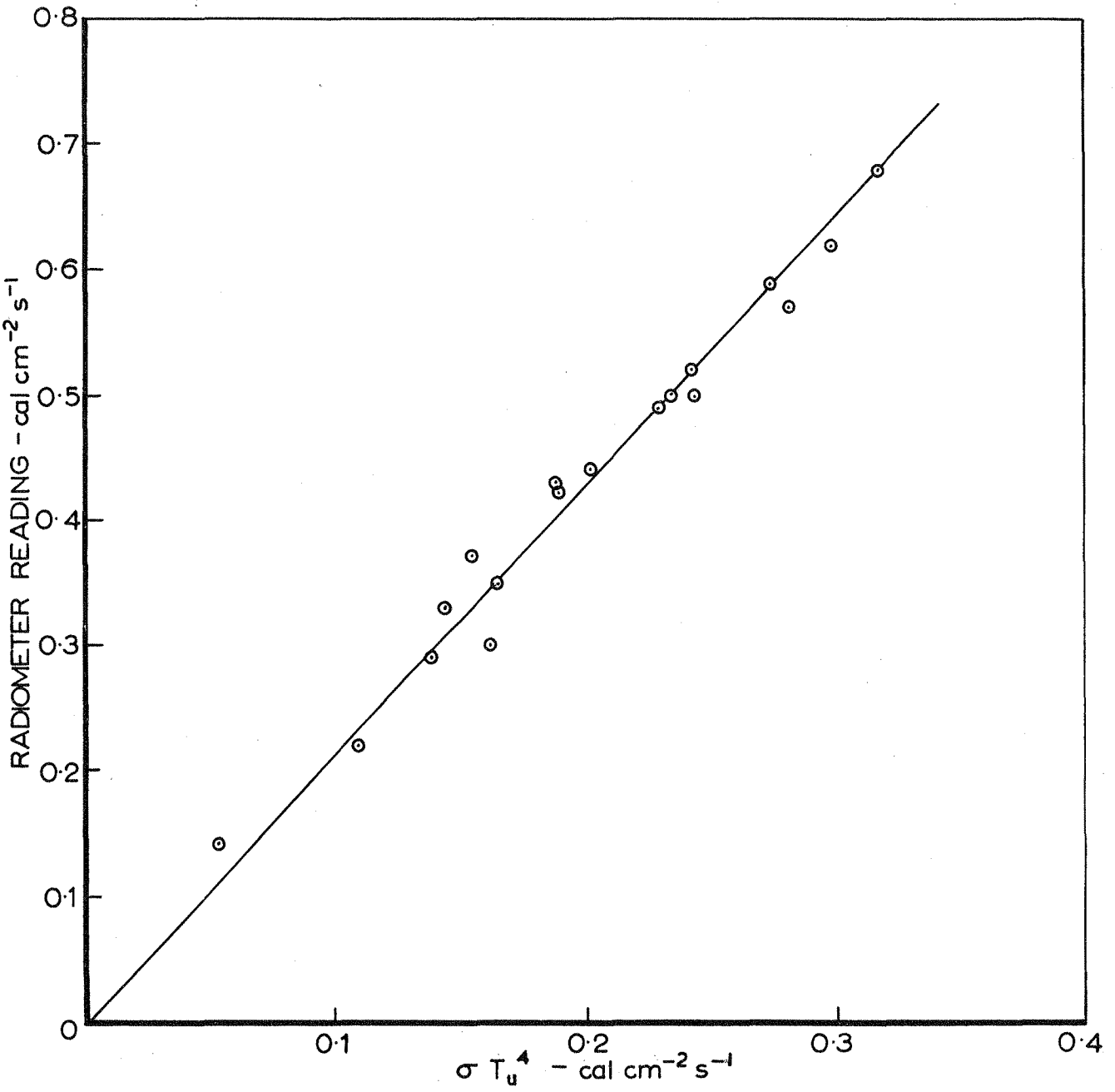

FIG. 11. RADIOMETER READING AGAINST σ T$_u^4$

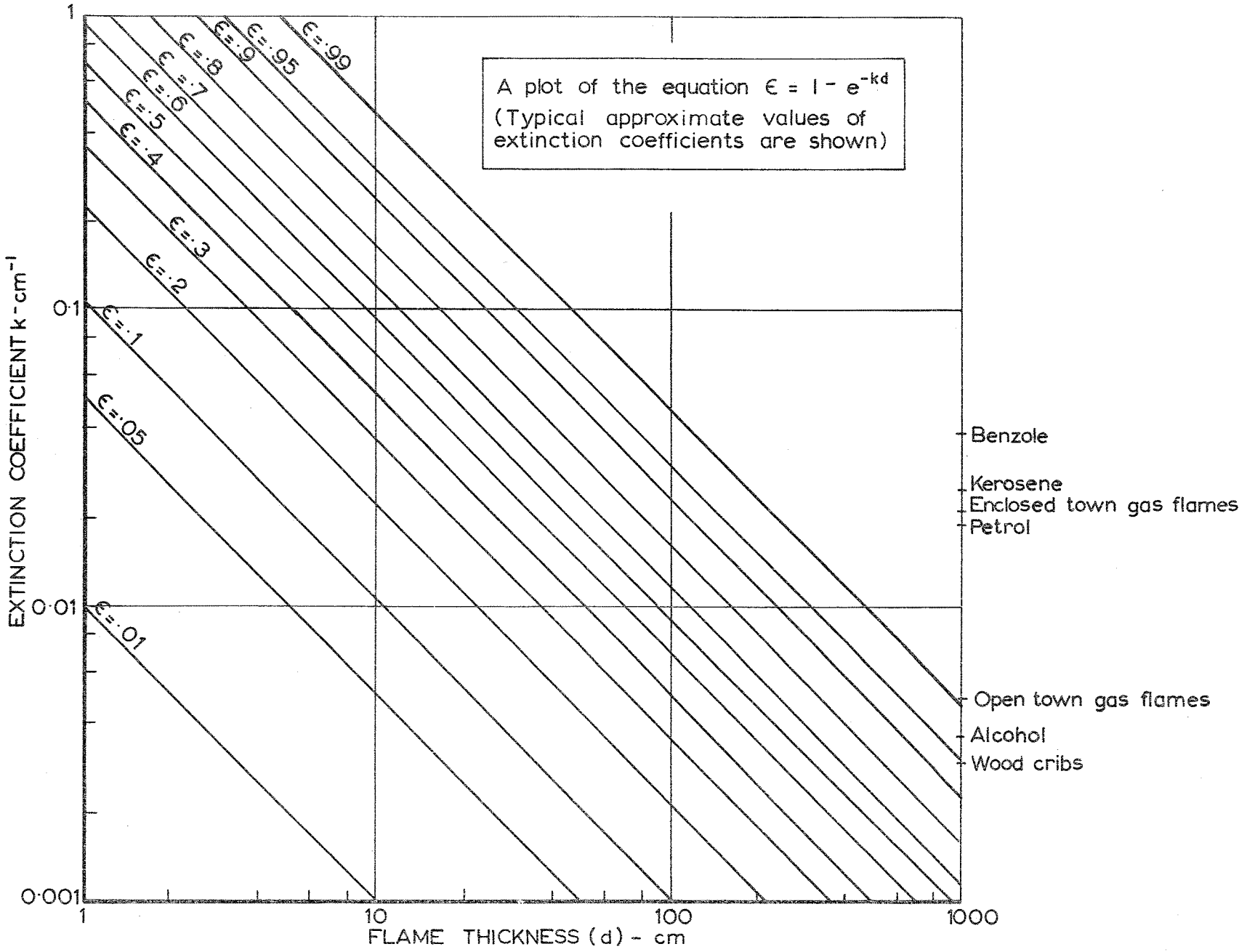

FIG. 12. FLAME EMISSIVITY AS A FUNCTION OF THICKNESS AND EXTINCTION COEFFICIENTS